Манассеро М., Доминианни А., Гварена Н. Использование геобентонитовых полотен для контроля загрязнения // Вестник ПНИПУ. Строительство и архитектура. – 2017. – Т. 8, № 4. – С. 126–140. DOI: 10.15593/2224-9826/2017.4.13

Manassero M., Dominijanni A., Guarena N. Use of geosynthetic clay liners for pollutant control. *Bulletin of PNRPU. Construction and Architecture*. 2017. Vol. 8, no. 4. Pp. 126-140. DOI: 10.15593/2224-9826/2017.4.13

ВЕСТНИК ПНИПУ.
СТРОИТЕЛЬСТВО И АРХИТЕКТУРА
Т. 8, № 4, 2017
PNRPU BULLETIN.
CONSTRUCTION AND ARCHITECTURE
http://vestnik.pstu.ru/arhit/about/inf/

DOI: 10.15593/2224-9826/2017.4.13
УДК 624.13

ИСПОЛЬЗОВАНИЕ ГЕОБЕНТОНИТОВЫХ ПОЛОТЕН ДЛЯ КОНТРОЛЯ ЗАГРЯЗНЕНИЯ

М. Манассеро, А. Доминианни, Н. Гварена

Политехнический университет Турина, Турин, Италия

О СТАТЬЕ

Получена: 04 июля 2017
Принята: 01 сентября 2017
Опубликована: 15 декабря 2017

Ключевые слова:

активные глины, микроструктура бентонита, химический осмос, состояние поверхности структуры, гидравлическая проводимость, барьеры полигонов депонирования, давление набухания

АННОТАЦИЯ

Осмотическая, гидравлическая и самовосстанавливающаяся эффективность барьеров на основе бентонита (например, геосинтетические глинистые вкладыши) для локализации загрязненных растворов регулируется как химико-физическими характеристиками, свойственными бентониту, такими как, например, плотность твердого тела (ρ_{sk}), общая удельная поверхностью (S) и общий фиксированный отрицательный электрический поверхностный заряд (σ), так и параметрами химико-механического состояния, способными количественно определять плотность скелета и структуру, т.е. общий (e) и nano (e_n) коэффициенты пористости, среднее количество пластин на агрегат (тактоид) ($N_{l,\,AV}$), эффективную концентрацию электрического фиксированного заряда ($\bar{c}_{sk,\,0}$) и фракцию Штерна (f_{Stern}). В свою очередь, при рассмотрении только насыщенных активных глин параметры состояния, по-видимому, контролируются историей эффективных напряжений (SH), ионной валентностью (v_i) и взаимосвязанной последовательностью воздействия концентрации солей в поровом растворе (c_s). Создана теоретическая основа, дающая возможность описывать химическое, гидравлическое и механическое поведение бентонитов в случае одномерных полей деформаций и течения. В частности, представлены отношения, связывающие вышеупомянутое состояние и свойственные рассматриваемому бентониту параметры с его гидравлической проводимостью (k), эффективный коэффициент диффузии (D_s^*), осмотический коэффициент (ω) и давление набухания (u_{sw}) при различных последовательностях историй нагружения и концентраций растворенного вещества. Предлагаемая теоретическая гидрохимико-механическая структура была подтверждена путем сопоставления ее прогнозов с некоторыми из имеющихся экспериментальных результатов по бентонитам (т.е. испытания на гидравлическую проводимость, испытаниями на набухание и тестами на осмотическую эффективность).

© **Марио Манассеро** – доктор наук, профессор, e-mail: mario.manassero@polito.it.
Андреа Доминианни – доктор наук, доцент, e-mail: andrea.dominijanni@polito.it.
Николо Гварена – магистр, e-mail: nicolo.guarena@polito.it.

Mario Manassero – Ph.D. in Geotechnical Engineering, Full Professor, e-mail: mario.manassero@polito.it.
Andrea Dominijanni – Ph.D. in Geotechnical Engineering, Associate Professor, e-mail: andrea.dominijanni@polito.it.
Nicolò Guarena – M.Sc. in Civil Engineering, Visiting Staff, e-mail: nicolo.guarena@polito.it.

USE OF GEOSYNTHETIC CLAY LINERS FOR POLLUTANT CONTROL

M. Manassero, A. Dominijanni, N. Guarena

Politecnico di Torino, Torino, Italy

ARTICLE INFO

Received: 04 July 2017
Accepted: 01 September 2017
Published: 15 December 2017

Keywords:

active clays, bentonite microstructure, chemico-osmosis, fabric state surface, hydraulic conductivity, landfill barriers, swelling pressure

ABSTRACT

The osmotic, hydraulic and self-healing efficiency of bentonite based barriers (e.g. geosynthetic clay liners) for containment of polluting solutes are governed both by the chemico-physical intrinsic parameters of the bentonite, i.e. the solid density (ρ_{sk}), the total specific surface (S), and the total fixed negative electric surface charge (σ), and by the chemico-mechanical state parameters able to quantify the solid skeleton density and fabric, i.e. the total (e) and nano (e_n) void ratio, the average number of platelets per tactoid ($N_{l,AV}$), the effective electric fixed-charge concentration ($\bar{c}_{sk,0}'$), and the Stern fraction (f_{Stern}). In turn, looking at saturated active clays only, the state parameters seem to be controlled by the effective stress history (SH), ionic valence (v_i) and related exposure sequence of salt concentrations in the pore solution (c_s). A theoretical framework, able to describe chemical, hydraulic and mechanical behaviours of bentonites in the case of one-dimensional strain and flow fields, has been set up. In particular, the relationships, linking the aforementioned state and intrinsic parameters of a given bentonite with its hydraulic conductivity (k), effective diffusion coefficient (D_s^*), osmotic coefficient (ω) and swelling pressure (u_{sw}) under different stress-histories and solute concentration sequences, are presented. The proposed theoretical hydro-chemico-mechanical framework has been validated by comparison of its predictions with some of the available experimental results on bentonites (i.e. hydraulic conductivity tests, swelling pressure tests and osmotic efficiency tests).

Bentonite structure

Bentonite is a clay soil that usually contains a significant percentage (e.g., ≥ 70 %) of the three-layered (2:1) clay mineral montmorillonite. Isomorphic substitution in montmorillonite usually results in the replacement of a portion of tetravalent silicon (Si^{4+}) and trivalent aluminium (Al^{3+}) in the crystalline structure with a divalent metal, such as magnesium (Mg^{2+}), and this leads to a negative surface charge. The ideal unit cell formula of montmorillonite is: $\{(OH)_4Si_8Al_{3.44}Mg_{0.66}O_{20}\cdot nH_2O^{0.66-}\}$, with an average surface charge of 0.66 equivalent per unit cell. Montmorillonite crystals consist of parallel-aligned, alumino-silicate lamellae, which are approximately 1 nm thick and 100–200 nm in the lateral extent. The unit cell parameters are 0.517 nm and 0.895 nm, which correspond to a unit cell area of 0.925 nm^2, or one unit charge per 1.4 nm^2. The corresponding surface charge, σ, is equal to 0.114 $C\cdot m^{-2}$. The total specific surface of a single platelet, S, available for water adsorption is approximately equal to 760 $m^2\cdot g^{-1}$, assuming a solid density, ρ_{sk}, of 2.65 $Mg\cdot m^{-3}$ or a specific gravity, G_s, of 2.65 (–).

Montmorillonite particles can be represented as infinitely extended platy particles, also called platelets or lamellae. The half distance, b, between the montmorillonite particles can be estimated from the total void ratio, e. Norrish [1] showed that bentonite can have a dispersed structure or fabric in which clay particles are present as well separated units, or an aggregated structure that consists of packets of particles, or tactoids, within which several clay platelets are in a parallel array, with a characteristic interparticle distance of 0.9 nm.

The formation of tactoids has the net result of reducing the surface area of the montmorillonite, which then behaves like a much larger particle with the diffuse double layer only fully manifesting itself on the outside surfaces. The formation of tactoids is due to internal flocculation of the clay platelets, and mainly depends on the concentration and the valence of the ions in the soil solution and, to a lesser extent, on the effective isotropic stress history or, in turn, on the total

void ratio, *e*. The average number of clay platelets or lamellae forming tactoids, $N_{l,\,AV}$, increases with an increase in the ion concentration and valence of cations in the soil solution, whereas there is not apparent unique trend in $N_{l,\,AV}$ versus the micro void ratio, e_m, for a given concentration. Unfortunately, the average number of platelets per tactoid is a very difficult parameter to be experimentally assessed by both direct (e.g. Nuclear Magnetic Resonance, X-ray Diffraction, Small Angle X-ray Spectrometry, Transmission Electron Microscopy) and indirect methods (e.g. Hydraulic Conductivity, Swelling, Osmosis, Anion Available Pore Volume); therefore, the possibility to link, for a given bentonite, the latter parameter to the total void ratio, *e*, and to the salt concentration of the equilibrium solution, c_s, can be considered a really important step forward to enhance the bentonite barriers design, as shown in the following of this paper.

The average half spacing, *b*, in perfectly dispersed clays may be estimated, assuming a uniform distribution of the clay platelets in a parallel orientation (Dominijanni and Manassero) [2] from the relation:

$$b = \frac{e}{\rho_{sk} S}. \tag{1}$$

If the clay has an aggregated structure, only the external surface of the tactoids is in contact with the mobile fluid, therefore the void space within the platelets in the tactoids should be subtracted from the total void space to obtain the micro-void space, e_m, with reference to the conducting pores (Dominijanni and Manassero) [2]. If $N_{l,\,AV}$ is the average number of platelets per tactoid, the external or effective specific surface, S_{eff}, and the internal specific surface, S_n, are given by:

$$S_{eff} = \frac{S}{N_{l,\,AV}}, \tag{2a}$$

$$S_n = S - S_{eff} = \frac{(N_{l,\,AV} - 1)}{N_{l,\,AV}} S. \tag{2b}$$

The average half spacing between the platelets in the tactoid, b_n, as determined by means of X-ray measurements, can vary between 0.2 nm and 0.5 nm (Shainberg et al.) [3]. The total void ratio, *e*, of the bentonite is given by the sum of the void ratio inside the tactoid representing the nano or non-conductive pores (nm size), e_n, and the void ratio representing the micro or conductive pores (μm size), e_m. The water inside the tactoids together with the water of the Stern Layer can be considered part of the solid particles and is excluded from the transport mechanisms.

Therefore, if d_d is the thickness of the Stern Layer consisting of hydrated cations wrapping the external surface of the tactoid, d_{Stern}, divided by the average half spacing between the platelets in the tactoid, b_n, the void ratio associated with the internal surfaces of the tactoid, e_n, can be estimated as follows:

$$e_n = b_n \rho_{sk} (S_n + \frac{S \cdot d_d}{N_{l,\,AV}}), \tag{3}$$

where ρ_{sk} = density of the solid particles. The corrected half spacing, b_m, between the tactoids, in the case of an aggregate microstructure of bentonite, can be estimated from an equation similar to Eq.1, or:

$$b_m = \frac{e_m}{\rho_{sk} S_{eff}}, \tag{4}$$

where $e_m = e - e_n$ = void ratio representing the void space between the tactoids.

For a given total void ratio, e, when $d_d > 1$ and the number of clay platelets in the tactoids, $N_{l,AV}$, increases, the external specific surface decreases and the void ratio, e_m, representing the pore volume available for the solute and solvent transport, increases. In contrast, e_m decreases when $d_d < 1$ and, as in the previous case, $N_{l,AV}$ increases and the external specific surface decreases.

Guyonnet et al. [4], through a comparison of the results of hydraulic conductivity tests and microscopic analyses of bentonite structure based on small angle X-ray scattering and transmission electron microscopy, showed that high values of the hydraulic conductivity are related to an aggregated fabric (also called the hydrated-solid phase), while low values of the hydraulic conductivity are related to a dispersed fabric (also called the gel phase). These experimental results can be explained by the increase in the average micro-pore size, due to tactoid formation as discussed subsequently in this paper.

State parameters

Referring to the conceptual scheme and the possible evolutions of the bentonite fabric previously described, other state parameters can be derived from the basic average number of platelets per tactoid, $N_{l,AV}$. Equation (2a) gives the effective specific surface, S_{eff}, based on the single platelet specific surface, S (= 760 $m^2 \cdot g^{-1}$), and the basic state parameter $N_{l,AV}$. Moreover, another useful state parameter can be directly derived from the latter through the following equation (see also Dominijanni et al.) [5]:

$$\overline{c}_{sk,0} = \frac{(1 - f_{Stern}) \cdot \sigma}{F} \cdot \rho_{sk} \cdot S_{eff}, \tag{5}$$

where: $\overline{c}_{sk,0}$ = effective fixed charge concentration of the solid skeleton relative to the solid volume (mol·m^{-3}); f_{Stern} = fraction of electric charge compensated by the cations specifically adsorbed in the Stern Layer ranging between 0.70 and 0.95 (–), and F = Faraday's constant (= 96.485 C·mol^{-1}). The proposed state parameters can be influenced primarily by the concentration of ions in the pore solution and by the void ratio, related in turn to the effective isotropic component of the stress history of the considered bentonite.

Once the family of chemical state parameters describing the bentonite fabric at the nano and micro scale have been defined, a parallel development can be drawn with some aspects of the well known elasto-plastic-work-hardening models within the traditional soil mechanics (e.g. the Cam Clay model) that are capable of simulating the mechanical behaviour of soils on the basis of a series of intrinsic and state parameters as reported in table 1.

Table 1

Intrinsic and state parameters for mechanical and chemical models

Fields	Actions	Intrinsic parameters	State parameters
Mechanical	Shear stress: τ	ρ_{sk}, φ_{cv}	e, p', ψ
Chemical	Ion concentration: c_s	S, σ	$N_{l,AV}$, S_{eff}, $\overline{c}_{sk,0}$, f_{Stern}, d_{Stern}

Notes: p' = isotropic effective stress component; ψ = dilatancy angle; φ_{cv} = friction angle at the critical state.

As shown in Dominijanni and Manassero [2, 6], the framework that includes the aforementioned chemical parameters is able to link the coupled transport phenomena of water and ions by imposing the chemical equilibrium between the bulk electrolyte solutions and the internal micro-pore solution at the macroscopic scale level, through the Donnan, Navier – Stokes and Nernst-Planck equations. Moreover, also some specific aspects of the mechanical behaviour can be modelled and coupled with

the chemical and transport behaviour by taking into account the different types of intergranular actions, beyond the solid contact stress and the bulk pore pressure (Terzaghi) [7], such as electromagnetic attraction/repulsion and osmotic swelling/suction forces (Mitchell and Soga) [8].

In principle, and similar to the evolution of the basic Cam Clay model by Alonso et al. [9] through the UPC model for unsaturated soil, the intrinsic and state parameters listed in Table 1 and the related framework can extend the basic theoretical approaches to include the mechanical behaviour that is related to the fabric of the active fine grained soils under fully saturated conditions, taking into account not only actions such as the stress history and the related void ratio, but also the ion species and the concentration changes in the pore fluids.

In the following discussion, the developed framework is applied to interpret some experimental results from the literature and from the authors' own laboratory testing, showing how the framework provides insight into the physico-chemico mechanisms that determine the observed macro-scale behaviour of active clays.

Validation of the solute transport and swelling Model

In order to implement an accurate validation of the proposed theoretical framework, Dominijanni and Manassero [10], Dominijanni et al. [11], and Manassero and Dominijanni [12] proposed a model obtained by upscaling the modified Navier-Stokes equation and the Nernst-Plank equations and using the Donnan equations to impose the chemical equilibrium between the bulk electrolyte solutions and the internal micro-pore solution. The proposed model provided a satisfactory interpretation of the experimental results of Malusis and Shackelford [13, 14], Malusis et al. [15] and Dominijanni et al. [5] in terms of osmotic efficiency, ω, of two bentonites (see tables 2 and 3 and figure 1) tested with solutions characterized by salt (KCl, NaCl) concentrations up to a maximum of c_s = 100 mM. The experimental data are in good agreement with the linear relationship, predicted by the theoretical model, relating the restrictive tortuosity factor, τ_r, to the osmotic efficiency coefficient, ω, as follows:

$$\tau_r = 1 - \omega, \tag{6}$$

where τ_r represents the ratio between the osmotic effective diffusion coefficient, D_ω^*, that is measured during an osmotic test (Malusis et al. [16]; Malusis and Shackelford [14]; Dominijanni et al. [5]) and the effective salt diffusion coefficient, D_S^*, that is obtained by extrapolating the value of D_ω^* at ω = 0.

Table 2

Physical and chemical intrinsic properties of the considered bentonites

	Dominijanni et al. [4], Puma et al. [21] and Boffa et al. [22]	Malusis and Shackelford [13, 14]	Seiphoori [27] and Manca [24]	Mazzieri et al. [25, 26]	Di Emidio [23]
Liquid limit, *LL* (%)	525	478	420	530	650
Plasticity index, *PI* (%)	–	439	355	480	600
Specific gravity, G_s (-)	2.65	2.43	2.74	2.65	2.66
Principal minerals (%):					
montmorillonite	98	71	85	90	95
quartz	–	15	4	–	–
other	–	7	11	–	–
Cation exchange capacity, *CEC* (meq/100g)	105	47.7	74.0	94.5	44.5

Table 3

Range of physical and state parameters of the bentonites in contact with deionized water and NaCl, KCl and $CaCl_2$ solutions

	Dominijanni et al. [4], Puma et al. [21] and Boffa et al. [22]	Malusis and Shackelford [13, 14]	Seiphoori [27] and Manca [24]	Mazzieri et al. [25, 26]	Di Emidio [23]	Dominijanni et al. [4], Puma et al. [21] and Boffa et al. [22]
Hydraulic Conductivity, k (m/s)	$6.00 \cdot 10^{-12}$ $1.20 \cdot 10^{-10}$	$1.63 \cdot 10^{-11}$	$1.0 \cdot 10^{-14}$ $1.0 \cdot 10^{-13}$	$1.6 \cdot 10^{-11}$ $2.2 \cdot 10^{-8}$	$6.5 \cdot 10^{-11}$	$6.42 \cdot 10^{-12}$
Steric Tortuosity Factor, τ_m (–)	0.30 0.36	0.14	0.20	0.30 0.50	0.35	0.35
Total Void Ratio, e_{tot} (–)	0.60 4.50	3.76	0.53 1.20	2.15 5.40	5.13	2.55
Micro Void Ratio, e_m (–)	0.10 2.99	2.56	0.05 0.38	1.23 4.35	3.6	1.13
Effective Diffusion Coefficient, D_s^* (m^2/s)	$5.0 \cdot 10^{-10}$	$2.7 \cdot 10^{-10}$	–	–	–	–
Osmotic Efficiency, ω (–)	0.00 0.68	0.35	–	–	–	–
Effective Specific Surface, S_{eff} (m^2/g)	24.14 216.71	164.40	36.18 92.15	6.09 121.81	159.65	129.94
Average Number of Platelets per Tactoid, $N_{l,AV}$ (–)	3.5 31.5	3.6	5.7 14.5	4.3 85.9	5.0	6.2
Stern Coefficient, f_{Stern} (–)	0.80 0.90	0.90	0.70	0.85	0.80	0,9
Fixed Charge Concentration, $\bar{c}_{sk,0}$ (M)	0.008 0.076	0.046	0.035 0.089	0.003 0.059	0.100	0.041

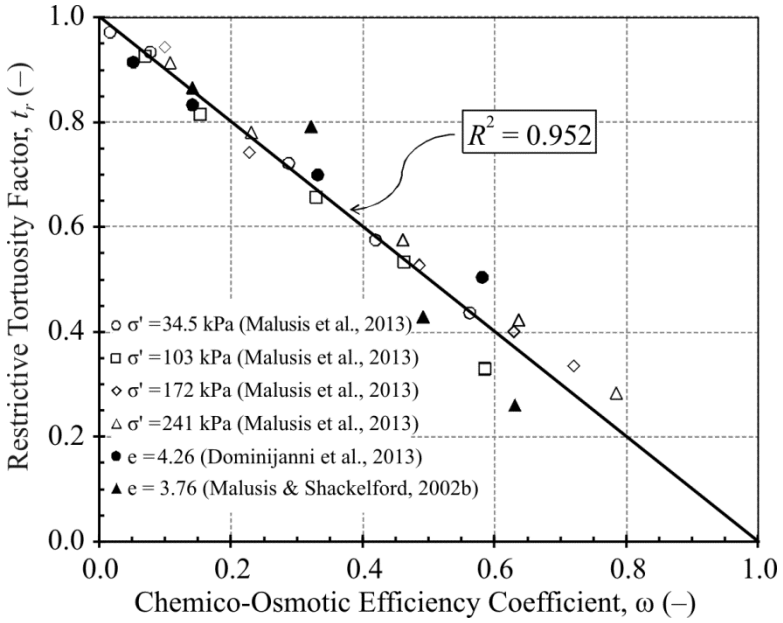

Fig. 1. Restrictive tortuosity factor versus chemico-osmotic efficiency coefficient with the theoretical linear relation

Also, the evaluation of the osmotic swelling pressure theoretically calculated on these samples by the use of the same input parameters, referring in particular to $N_{l,AV}$, S_{eff}, $\bar{c}_{sk,0}$, was in very good agreement with the related experimental results (see Manassero et al. [17]). However,

the range of salt concentrations, c_s, investigated within the experimental tests previously noted, was not sufficient to induce any significant variation in bentonite fabric and, therefore, the values of the defined fabric state parameters ($N_{l,AV}$, S_{eff} and $\bar{c}_{sk,0}$).

For this reason, a more general and reliable validation of the proposed theoretical framework for modelling the bentonite hydro-chemico-mechanical behaviour requires consideration of other experimental results, such as both the hydraulic conductivity and the swelling pressure, using ion concentrations higher than 200 mM and, possibly, ≥ 1000 mM. In the case of the higher ion concentrations, the fabric of the bentonites undergoes major changes due to flocculation phenomenon under low confining stress (high void ratio), resulting in a significant increase in the average number of platelets per tactoid and a correspondent decrease in the effective specific surface and fixed charge concentration of the solid skeleton, as summarized in table 4.

Table 4

Ranges of variation of monovalent ion equivalent concentrations
that influence the main performance parameters of bentonites

Main performance parameters of bentonite barriers	Ranges of monovalent ion concentration, c_s [mM]	Notes
Osmotic efficiency, ω	0–100	No fabric variation. For c_s higher than 100 mM ω = 0
Swelling pressure, u_{sw}	0–200	Small fabric variation. For c_s around 200 mM u_{sw} = 0
Hydraulic conductivity, k	200–5000	Significant fabric variation and significant k increments
Steric tortuosity factor, τ_m	200–5000	Significant fabric variation and significant τ_m increments

A series of hydraulic conductivity, swelling and oedometer tests performed on different bentonites by different authors (see table 2, 3) have been analysed to validate the proposed general framework. The comparison of experimental and theoretical results consists of the following steps:

– Referring to a first series of hydraulic conductivity tests on different bentonites and permeant solutions, an assessment of the effective specific surface, S_{eff}, has been performed using the following equation (Kozeny [18]; Carman [19]; Dominijanni et al. [5]):

$$k = \frac{\tau_m}{3} \frac{e_m^3}{(1+e_m)\cdot(\mu_w + \mu_{ev})} \frac{\gamma_w}{(\rho_{sk} S_{eff})^2}. \tag{7}$$

Neglecting as a first approximation the electro-viscosity coefficient, μ_{ev}, the definitions of the remaining undefined terms are: τ_m = matrix or steric tortuosity factor (≤ 1) that takes into account the tortuous nature of the actual permeant pathways through the porous medium due to the geometry of the interconnected pores, μ_w = water viscosity coefficient, and γ_w = water unit weight.

– The evaluation of the average number of platelets per tactoid, $N_{l,AV}$, and $\bar{c}_{sk,0}$ has been carried out via Eqs. 2a and 5, respectively, and the assessment of the theoretical results in terms of swelling pressure, u_{sw}, has been obtained as follows (from Dominijanni et al. [5]):

$$u_{sw} = 2RTc_s \left[\sqrt{\left(\frac{\bar{c}_{sk,0}}{2e_m \cdot c_s} \right)^2 + 1} - 1 \right], \tag{8}$$

where R is the ideal gas constant and T is the absolute temperature (K). The comparisons of the latter with the experimental swelling test results for the same bentonite samples are plotted in figure 2.

– An additional assessment of the reliability of the proposed theoretical model, with reference to Eq. 8, is shown in figure 3, where all the swelling and oedometer test results in terms of swelling pressure of the samples permeated or hydrated with deionized water or low concentration solutions ($c_s \leq 10$ mM) are shown together with the obtained theoretical trend.

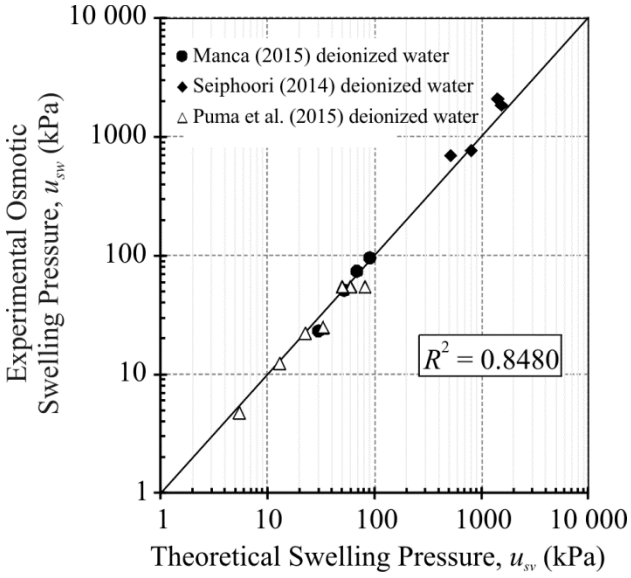

Fig. 2. Experimental versus theoretical swelling pressure using input state parameters from hydraulic conductivity tests

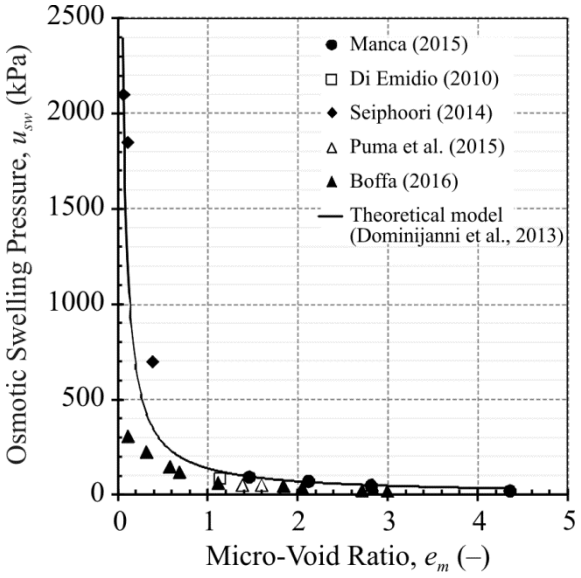

Fig. 3. Swelling pressure versus micro-void ratio for samples tested with deionized water and solutions with monovalent ion equivalent concentration $c_s \leq 10$ mM

Finally, all the available bentonite samples, in contact with both deionized water and different chemical solutions, have been considered for the assessment of the basic state parameter, $N_{l,\,AV}$, throughout the experimental hydraulic conductivity and swelling pressure measurements. This parameter is uniquely linked with the other two electro-fabric state parameters (i.e. S_{eff}, $\overline{c}_{sk,\,0}$) and, moreover, provides, as previously illustrated, a satisfactory prediction of chemico-osmotic, hydraulic and swelling/shrinking behaviours of bentonites. The obtained $N_{l,\,AV}$ values have been plotted versus the micro-void ratio, e_m, in fig. 4 and 5, with fig. 5 simply being the enlargement of the vertical axis close to the origin of fig. 4.

In order to relate $N_{l,\,AV}$ to e_m and c_s, the following phenomenological equation has been proposed:

$$N_{l,\,AV} = N_{l,\,AV0} + \frac{\alpha}{e_m} \cdot \left(\frac{c_s}{c_0} + 1 \right) + \beta \cdot e_m \cdot \left[1 - \exp\left(-\frac{c_s}{c_0} \right) \right], \tag{9}$$

where c_0 represents the reference concentration (= 1 M), $N_{l,\,AV0}$ is the ideal average minimum number of lamellae per tactoid when c_s = 0 and $e_m \rightarrow \infty$; $\alpha = e_m \cdot \left(N_{l,\,AV} - N_{l,\,AV0} \right)$ for c_s = 0 is a coefficient relating $N_{l,\,AV}$ and e_m when c_s = 0 and β is a constriction degree coefficient of the platelets. The parameters $N_{l,\,AV0}$ and β are both depending on bentonite type, pre-treatments (e.g. removal of soluble salts, consolidation), hydration and chemicals exposure sequence.

The micro-void ratio e_m in Eq. 9 can be derived from the total void ratio through the following equation:

$$e_m = \frac{e \cdot N_{l,\,AV} - S \rho_{sk} b_n \left(N_{l,\,AV} + d_d - 1 \right)}{N_{l,\,AV}}. \tag{10}$$

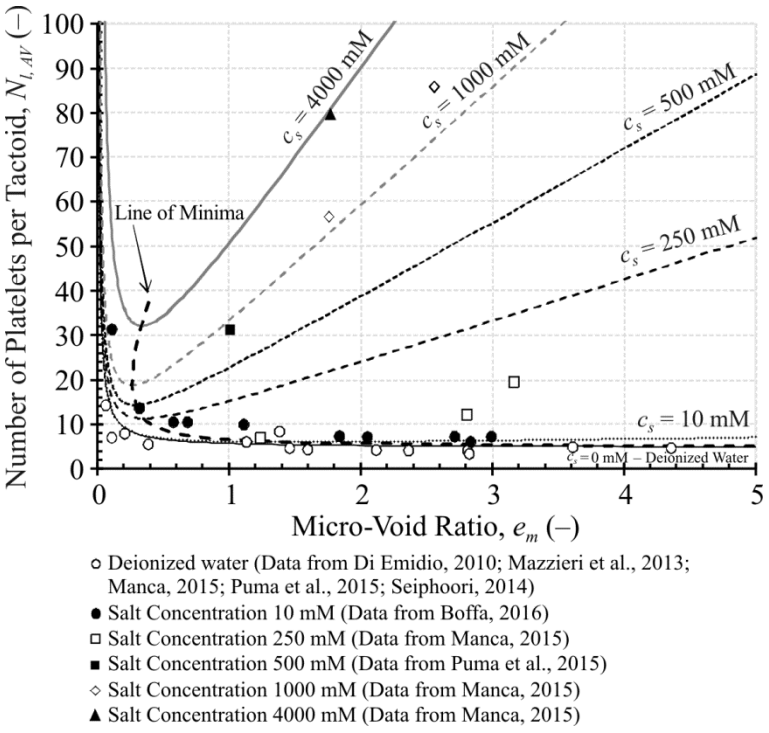

Fig. 4. Average number of platelets per tactoid ($N_{l,AV}$) versus micro void ratio (e_m) based on values from the interpretation of hydraulic conductivity, osmotic and swelling tests (Fitting parameters: $N_{l,AV0}$ = 4.79, α = 0.91, β = 42.45; coefficient of determination, R^2 = 0.89)

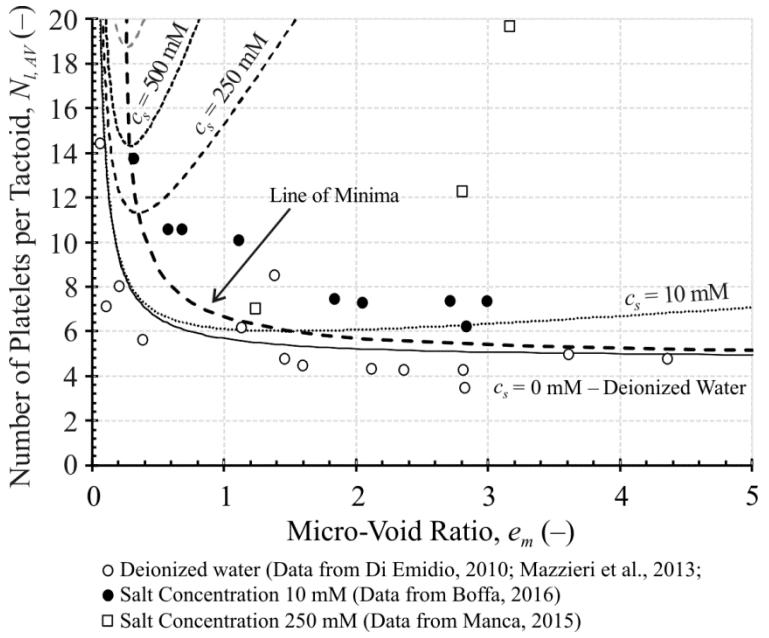

Fig. 5. Enlargement of Fig. 4 for the range $0 < N_{l,AV} < 20$

Inserting Eq. 10 into Eq. 9 the number of lamellae per tactoid is related to the total void ratio and the salt concentration through a cubic equation, which can be solved analytically or numerically for given values of the parameters $N_{l,AV0}$, α, β, S, ρ_{sk}, b_n and d_d.

All the available experimental data, previously mentioned, were regressed by imposing $N_{l,AV0}$ = 4.79, α = 0.91 and β = 42.45 (coefficient of determination, R^2 = 0.89).

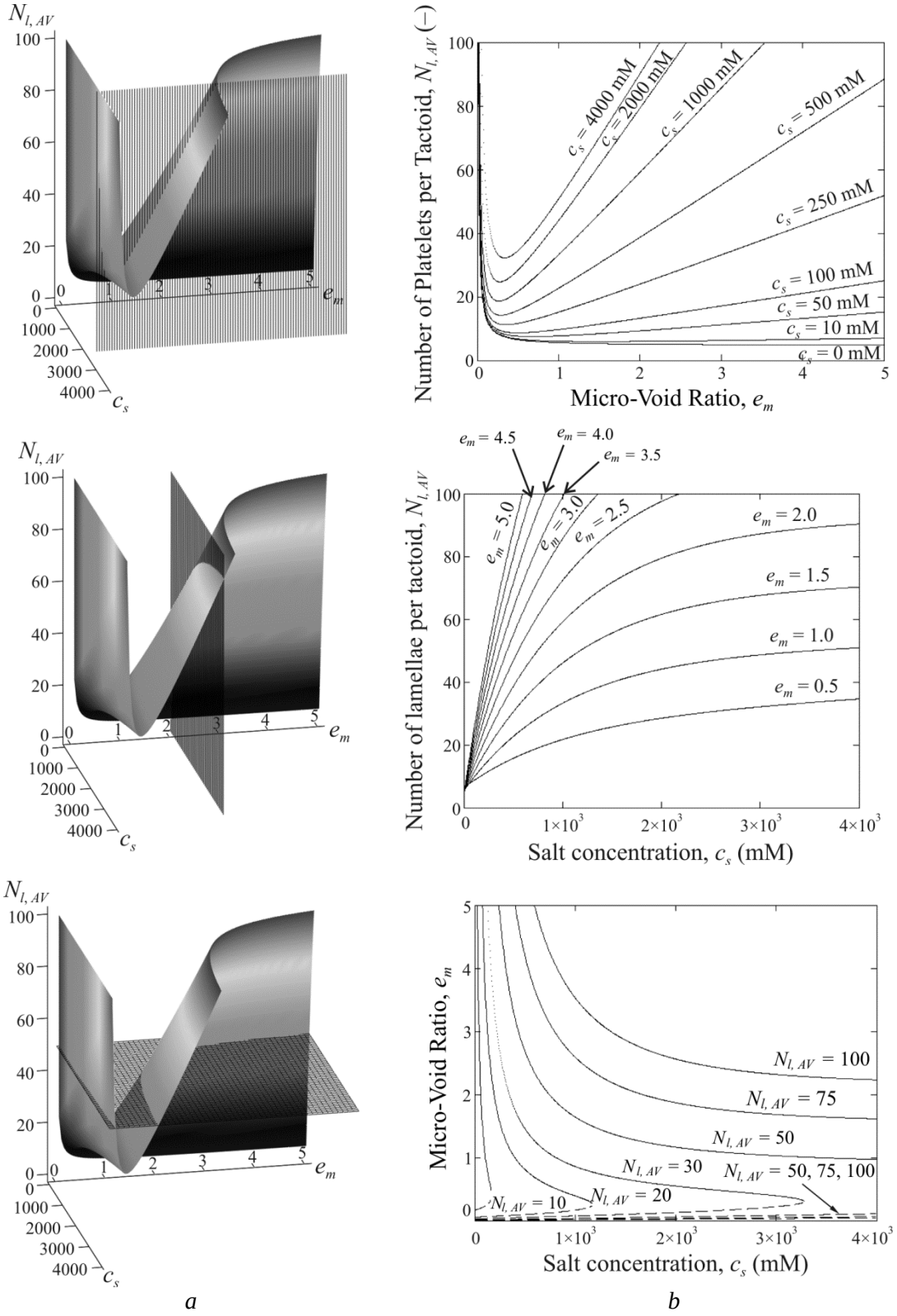

Fig. 6. 3D image of the Fabric State Surface (*a*); planar section traces of the Fabric State Surface (*b*)

It is now interesting to observe the regression results, in terms of average number of lamellae per tactoid, obtained from the interpretation of the aforementioned hydraulic conductivity and swelling tests. The average number of lamellae per tactoid plotted versus the micro void ratio (i.e. the inter-tactoids void ratio) in particular shows, as expected, a very interesting trend. In fact, for any given electrolyte concentration (apart from the unique case of deionized water), an initial decrease in $N_{l,\,AV}$ to a minimum value is followed by a continuous increasing trend with corresponding increase in the micro-void ratio.

More specifically, the ideal line, which represents the minimum loci of the aforementioned function at the different ion concentrations, c_s, of the solutions in contact with the bentonite versus e_m may represent a separation locus between flocculating and dispersive behaviour of the considered bentonites, in a similar way to the case of unsaturated soils where swelling and shrinking behaviours are dependent on the degree of saturation (or suction) versus the confining stress and related void ratio (Alonso et al. [9]).

Some 3D views of the proposed Fabric State Surface in the domain defined by the number of lamellae per tactoid, $N_{l,\,AV}$, the micro-void ratio, e_m, and the electrolyte concentration, c_s, are reported in Figure 6, together with the profiles defined by planar sections orthogonal to the main axes.

Application of the proposed model to the geosynthetic clay Liners (GCLs)

An additional validation of the proposed model has been performed referring to the experimental results provided by Petrov and Rowe [20] on a needle punched geosynthetic clay liner. The authors conducted hydraulic conductivity tests after a pre-hydration with distilled water. The tests covered a wide range of effective confining stresses (from 3.4 to 114 kPa) and concentrations of the permeant NaCl solutions (from 0.01 to 2.0 M), thus providing a sizeable range of data available for calibration. The intrinsic properties and state parameters of the GCL tested by Petrov and Rowe [20] are reported in Table 5. Incidentally, it has to be noted that, for this set of data, the interpretation via the same model parameters adjusted for natural bentonites may be incorrect conceptually, because of the potential impact resulting from the presence of the needle-punched fibres, which is expected to cause higher values of hydraulic conductivity due to the formation of preferential flow pathways along the fibres of the needling treatment when the GCL is permeated with solutions having a high salt concentration (Puma et al. [21]).

Table 5

Intrinsic properties and state parameters of the GCL tested by Petrov and Rowe [20] in contact with NaCl solutions

Physical and Chemical Intrinsic Properties		Range of Physical and State Parameters	
Montmorillonite Content, (%)	91	Hydraulic Conductivity, k (m/s)	$4.8\cdot10^{-12}$ $2.9\cdot10^{-9}$
Specific Gravity, G_s (–)	2.61	Total Void Ratio, e_{tot} (–)	1.60 4.89
Total Specific Surface, S (m^2/g)	750	Micro Void Ratio, e_m (–)	0.65 3.82
Cation Exchange Capacity, *CEC* (meq/100g)	85.8	Effective Specific Surface, S_{eff} (m2/g)	16.17 123.08
		Number of Platelets per Tactoid, $N_{l,\,AV}$ (–)	6.1 46.4
		Fixed Charge Concentration, $\overline{c}_{sk,\,0}$ (M)	0.007 0.057

In Figure 7 *a*, *b* and *c*, the ordinary least squares has been applied for the data regression which results in $N_{l,\,AV0}$ = 1.56, α = 8.82, β = 10.01, and a high coefficient of determination has been obtained (R^2 = 0.9384) as shown in Figure 8. These results highlight the reliability of the proposed equation of the Fabric State Surface, and its ability to simulate the coupled chemico-mechanical behaviour of active clays, once the fabric parameters have been properly assessed referring to the specific bentonite and related GCL to be modelled.

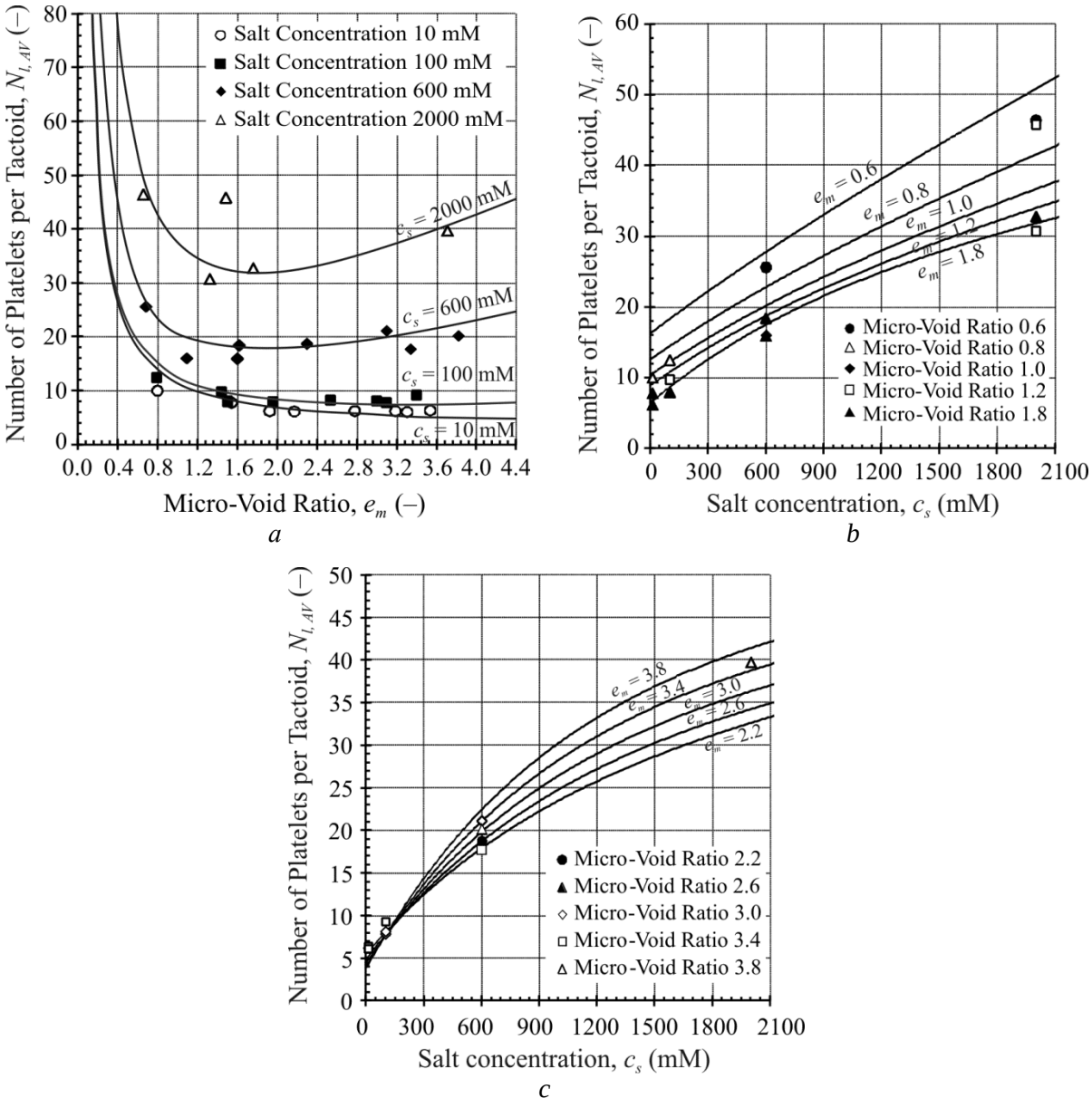

Fig. 7. Calibration of the parameters that define the Fabric State Surface on the experimental results given by Petrov and Rowe [20] ($N_{l,\,AV0}$ = 1.56, α = 8.82, β = 10.01): (*a*) $N_{l,\,AV}$ vs e_m; (*b*) $N_{l,\,AV}$ vs c_s; (*c*) $N_{l,\,AV}$ vs c_s

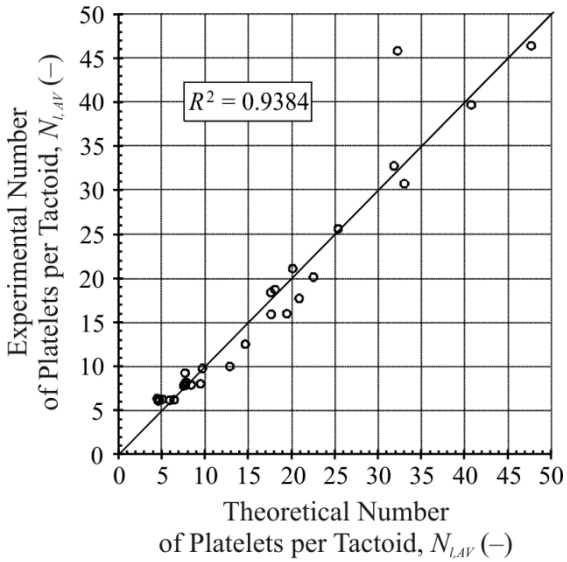

Fig. 8. Experimental versus theoretical average number of lamellae per tactoid $N_{l,AV}$, using the hydraulic conductivity data provided by Petrov and Rowe [20] and the related calibration of the fabric parameters

Conclusions

A series of chemico-fabric state parameters (i.e. effective specific surface, S_{eff}, average number of platelets per tactoid, $N_{l,AV}$, and solid skeleton electric fixed charge concentration, $\bar{c}_{sk,0}$) were defined to predict the chemico-osmotic, hydraulic, and swelling behaviour of bentonites currently used within typical geosynthetic clay liners (GCLs). Moreover, a theoretical model was presented, based on the state parameters listed over, and its capability to predict the main performances of bentonite barriers for pollutant control was assessed. The comparison of the theoretical results versus the experimental ones was very good.

Furthermore, plotting the average number of platelets per tactoid, $N_{l,AV}$, versus the micro-void ratio, e_m (i.e. the pore volume of the inter-tactoids), for different ion concentrations of the pore solutions, an interesting trend was observed. In fact, for any given ion concentration of the solution in contact with the bentonite (apart from deionized water), the value of $N_{l,AV}$, after an initial decrease and a minimum value, shows a continuous increasing trend with increase in the micro-void ratio.

A theoretical function has been proposed to relate the number of lamellae per tactoid with the micro-void ratio and the salt concentration. This function represents the state boundary surface of the chemical-mechanical coupled model. The ideal line, that represents the minimum loci of the aforementioned function at the different ion concentrations, c_s, of the solutions in contact with the bentonite versus e_m may represent a separation line between swelling and shrinking behaviours of the considered bentonites, similar to the case of unsaturated soils where the expanding and collapsible behaviours are dependent on the degree of saturation or suction versus the confining stress and/or void ratio (see Alonso et al. [9]).

However, further experimental studies must be implemented in order to corroborate the aforementioned theoretical framework. Nevertheless, some very interesting and useful knowledge can already be modelled in a reliable way and practically exploited for prediction and assessment of the performance of bentonite barriers with particular reference to geosynthetic clay liners (GCLs) for pollutant containment.

References

1. Norrish K. The swelling of montmorillonite. *Discussions of the Faraday Society*, *18*, 1954, pp. 120-134.

2. Dominijanni A., Manassero M. Modelling the swelling and osmotic properties of clay soils. Part II: The physical approach. *International Journal of Engineering Science*, 2012, no. 51, pp. 51-73.

3. Shainberg I., Bresler E., Klausner Y. Studies on Na/Ca montmorillonite systems. 1. The swelling pressure. *Soil Science*, no. 111(4), 1971, pp. 214-219.

4. Guyonnet D., Gaucher E., Gaboriau H., Pons C.H., Clinard C., Norotte V., Didier G. Geosynthetic clay liner interaction with leachate: correlation between permeability, microstructure and surface chemistry. *Journal of Geotechnical and Geoenvironmental Engineering*, no. 131(6), 2005, pp. 740-749.

5. Dominijanni A., Manassero M., Puma S. Coupled chemical-hydraulic-mechanical behavior of bentonites. *Géotechnique*, no. 63(3), 2013, pp. 191-205.

6. Dominijanni A., Manassero M. Modelling the swelling and osmotic properties of clay soils. Part I: The phenomenological approach. *International Journal of Engineering Science*, no. 51, 2012, pp. 32-50.

7. Terzaghi K. Theoretical soil mechanics. New York, John Wiley and Sons, 1943, 526 p.

8. Mitchell J.K., Soga K. Fundamentals of soil behavior. 3rd ed. New York, John Wiley and Sons, 2005, 592 p.

9. Alonso E., Gens A., Josa A. A constitutive model for partially saturated soils. *Géotechnique*, no. 40(3), 1990, pp. 405-430.

10. Dominijanni A., Manassero M. Modelling osmosis and solute transport through clay membrane barriers. *Waste Containment and Remediation. ASCE Geotechnical Special Publication*. Eds Alshawabkleh A. et al. ASCE, Reston/VA, 2005, No. 47.

11. Dominijanni A., Manassero M., Vanni D. Micro/macro modeling of electrolyte transport through semipermeable bentonite layers. *Proceedings of the 5th International Congress on Environmental Geotechnics*, 26th-30th June, Cardiff, Wales, UK, London, Thomas Telford, 2006, vol. II, pp. 1123-1130.

12. Manassero M., Dominijanni A. Coupled modelling of swelling properties and electrolyte transport through geosynthetic clay liner. *Proceedings of the Sixth International Congress on Environmental Geotechnics (6ICEG)*, 8-12 November, New Delhi, India, 2010, vol. 1, pp. 260-271.

13. Malusis M.A., Shackelford C.D. Chemico-osmotic efficiency of a geosynthetic clay liner. *Journal of Geotechnical and Geoenvironmental Engineering*, no. 128(2), 2002, pp. 97–106.

14. Malusis M.A., Shackelford C.D. Coupling effects during steady-state solute diffusion through a semipermeable clay membrane. *Environmental Science and Technology*, no. 36(6), 2002, pp. 1312–1319.

15. Malusis M., Kang J., Shackelford C.D. Influence of membrane behavior on solute diffusion through GCLs. *Proceedings of the International Symposium on Coupled Phenomena in Environmental Geotechnics (CPEG), ISSMGE TC 215*, 1-3 July, Torino (Italy) 2013, London, CRC Press Taylor & Francis Group, 2013, pp. 267-274.

16. Malusis M.A., Shackelford C.D., Olsen H.W. A laboratory apparatus to measure chemico-osmotic efficiency coefficients for clay soils. *Geotechnical Testing Journal*, no. 24(3), 2001, pp. 229–242.

17. Manassero M., Dominijanni A., Musso G., Puma S. Coupled phenomena in contaminant transport. Theme Lecture in. *Proceedings of the 7th International Congress on Environmental Geotechnics*, 10-14 November, Melbourne (Australia), 2014, pp. 144-169.

18. Kozeny J. Ueber kapillare Leitung des Wassers im Boden. Wien, Sitzungsbericht Akad. Wiss., no. 136(2a), 1927, pp. 271-306.

19. Carman P.C. Flow of gases through porous media. Butterworths, London, 1956.

20. Petrov R.J., Rowe R.K. Geosynthetic clay liner (GCL) – chemical compatibility by hydraulic conductivity testing and factors impacting its performance. Canadian Geotechnical Journal, 1997, 34, pp. 63-885.

21. Puma S., Dominijanni A., Manassero M., Zaninetta L. The role of physical pretreatments on the hydraulic conductivity of natural sodium bentonites. Geotextiles and Geomembranes, 2015, 43, pp. 263-271.

22. Boffa G., Dominijanni A., Manassero M., Marangon M., Zaninetta L. Mechanical and swelling behavior of sodium bentonites in equilibrium with low molarity NaCl solutions under oedometric conditions. Acta Geotechnica (under review), 2016.

23. Di Emidio G. Hydraulic and chemico-osmotic performance of polymer treated clays. Ph.D. Thesis, Ghent: Ghent University, 2010.

24. Manca D. Hydro-chemo-mechanical characterization of sand/bentonite mixtures, with focus on their water and gas transport properties. Ph.D. Thesis. EPFL, Lausanne (Switzerland), 2015.

25. Mazzieri F., Di Emidio G. Caratteristiche e prestazione di geocompositi bentonitici preidratati. In: Proceeding 24th Italian Geotechnical Conference, Napoli, June 2011, Ed. AGI, Rome: 735-742 (in Italian).

26. Mazzieri F., Di Emidio G., Fratalocchi E., Di Sante M., Pasqualini E. Permeation of two GCLs with an acidic metal-rich synthetic leachate. Geotextiles and Geomembranes, 2013, 40(10), pp. 1-11.

27. Seiphoori A. Thermo-hydro-mechanical characterization and modelling of MX-80 granular bentonite. Ph. D. Thesis n° 6159. EPFL, Lausanne (Switzerland), 2014.